CSaransh : Software Suite to Study Molecular Dynamics Simulations of Collision Cascades

Utkarsh Bhardwaj[1], **Harsh Hemani**[1], **Manoj Warrier**[1], **Nancy Semwal**[1], **Kawsar Ali**[1], **and Ashok Arya**[1]

1 Bhabha Atomic Research Center, India

Summary

The micro-structural properties of materials change due to irradiation. The defects formed during the displacement cascades caused by irradiation are the primary source of radiation damage (Björkas, Nordlund, & Caturla, 2012; Stoller, 2012). The number of primary defects produced, defect cluster size distribution, and defect cluster structures after a collision cascade can be studied using Molecular Dynamics simulations. These results determine the long term evolution of the micro-structural changes in the material (Becquart et al., 2006; Golubov, Singh, & Trinkaus, 2000; Osetsky, Bacon, Serra, Singh, & Golubov, 2000; Singh et al., 1997; Stoller, 2012). The properties studied using Molecular Dynamics (MD) simulations can be used in higher scale radiation damage models like Monte Carlo methods and rate theories. (Becquart et al., 2006; Osetsky et al., 2000).

CSaransh is a software suite to explore the Molecular Dynamics simulations of collision cascades. It includes post-processors to identify defects, characterize and classify cluster-structures, find number of sub-cascades etc. and a single page web-application (SPA) as GUI that provides interactive visualizations and charts such as:

- Different 3D-visualizations for a cascade including heat-maps, sub-cascades view, clusters-view.
- Interactive tool for pattern matching of cluster structures across the database.
- Charts for comparison of properties of cascades such as cluster size distribution, spatial and angular distribution of defects from primary knock-on position.
- Statistical analysis over elements and energies and correlations for all the cascades for the properties like number of defects, dimensionality of cascades, number of sub-cascades etc.
- Interactive tool for exploring the classes identified for the clusters found.

With the combination of efficient algorithms, unsupervised machine learning and modern interactive GUI with 3D visualizations the application helps in exploring different aspects of collision cascades qualitatively as well as quantitatively. Using the application many interesting correlations and patterns specific to different materials or energy ranges can be explored. We developed an efficient algorithm to identify defects from big MD simulation files. We use statistics and various unsupervised machine learning algorithms like HDBSCAN (Campello, Moulavi, & Sander, 2013), UMAP (McInnes & Healy, 2018), PCA to find various features such as identification of sub-cascades, characterization and classification of cluster structures based on features we have developed, identifying dimensionality of cascades and clusters.

The suite uses different tools for various tasks according to suitability. C++14 is used to efficiently post-process big simulation outputs. Python is used to add properties found using machine learning algorithms. HTML with React-js (Facebook, 2013) is used to develop the single page application. The charting libraries, chart-js (Chartjs, 2014) and plotly.js (Plotly, 2013) are used for the different charts. JSON is used as the common data format between

post-processors and GUI.

The CSaransh application was an entry in the IAEA challenge on Materials For Fusion, 2018 (IAEA, 2018). The description of the new algorithms for identification of defects and classification of clusters can be found in the arXiv paper (Bhardwaj, Sand, & Warrier, 2018). A talk in MoD-PMI 2019 workshop (Bhardwaj, Sand, & Warrier, 2019) was presented on the same topic.

The application shows results on data from the IAEA challenge as the default view, however any simulation data can be then loaded to study and explore. The application is planned to be included for the exploration of CascadesDB database (Hill, 2018).

Screenshots

		Inputs				Output Defects Information					
Actions	Material	Energy (keV)	PKA (θ)	PKA (φ)	Defects Count	Max clust...	% Defect...	1D-variance	2D-variance	Subcasde...	Impact m...
	×Fe ×W × ▼	×50 ×100 × ▼	30 — 169	1 — 90	0 — 242	0 — 158	0 — 92	0 — 87	0 — 98	0 — 5	0 — 97
👁◉	Fe	100	73.349	12.275	241	126	71.1618	80	95	1	30
👁◉	Fe	100	113.207	68.759	156	23	53.5256	71	97	3	96
👁◉	Fe	100	78.421	49.032	211	78	68.0095	86	96	2	51
👁🚫	Fe	100	163.349	57.06	137	6	35.4015	66	92	5	100
👁◉	Fe	100	103.64	16.684	192	41	54.9479	81	95	4	37

Figure 1: Main table with reactive filters, sorting and selection. The cascades of interest can be chosen here using the first (view) action button placed in first column of each row. Filters and sorting can be applied using the sliders for energy, directions, defects count, etc. The statistics are shown for only the filtered rows. To exclude a single row from the statistics, the second action button for that row can be toggled.
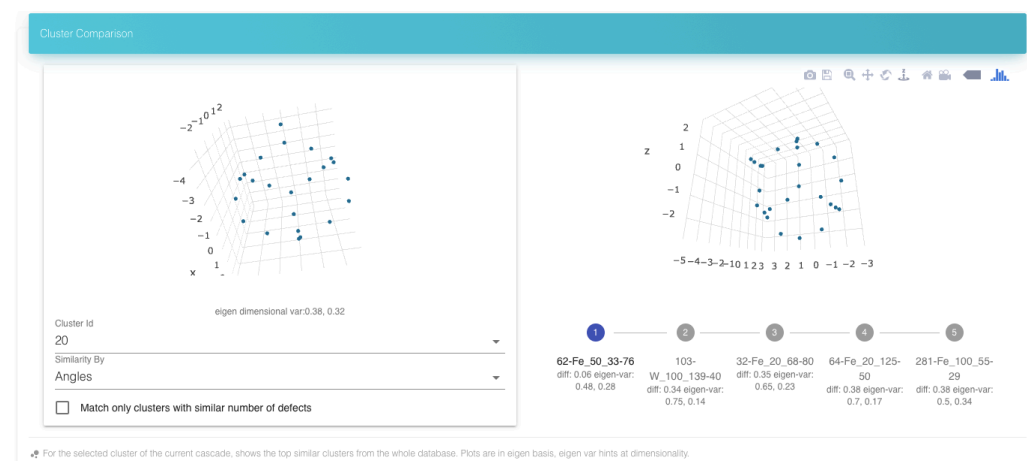

Figure 2: Section to choose and compare similar clusters. The cluster of interest can be chosen from the cascade view or the list on the left. The right side shows the top five clusters from the complete database of cascades that match the shape of the cluster on the left. There are different matching criteria to choose from. Each of the matches can be separately viewed by clicking on the choices displayed on the bottom of the right section along with the (dis-)similarity metric from the cluster on left and dimensionality.
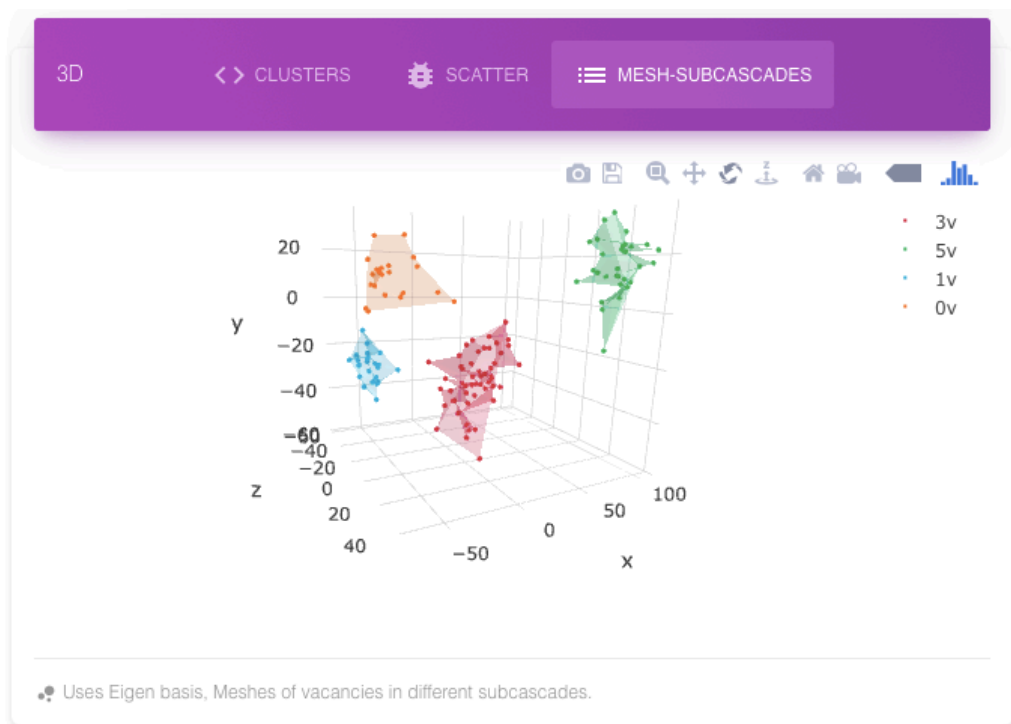
Figure 3: A high energy cascade can be composed of different sub-cascades or fragments. The sub-cascades are found using the DBSCAN algorithm on the vacancies created in the cascade.
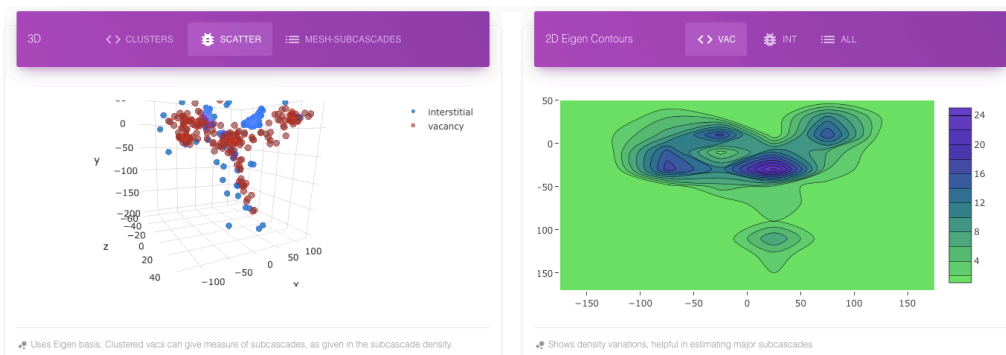

Figure 4: Scatter view and heat-map view for the same cascade. Heat map can be viewed for the vacancies, interstitials and both. It represents the density of defects. The scatter view and specifically heat map for vacancies can give a qualitative idea of the sub-cascading and range of the cascade.
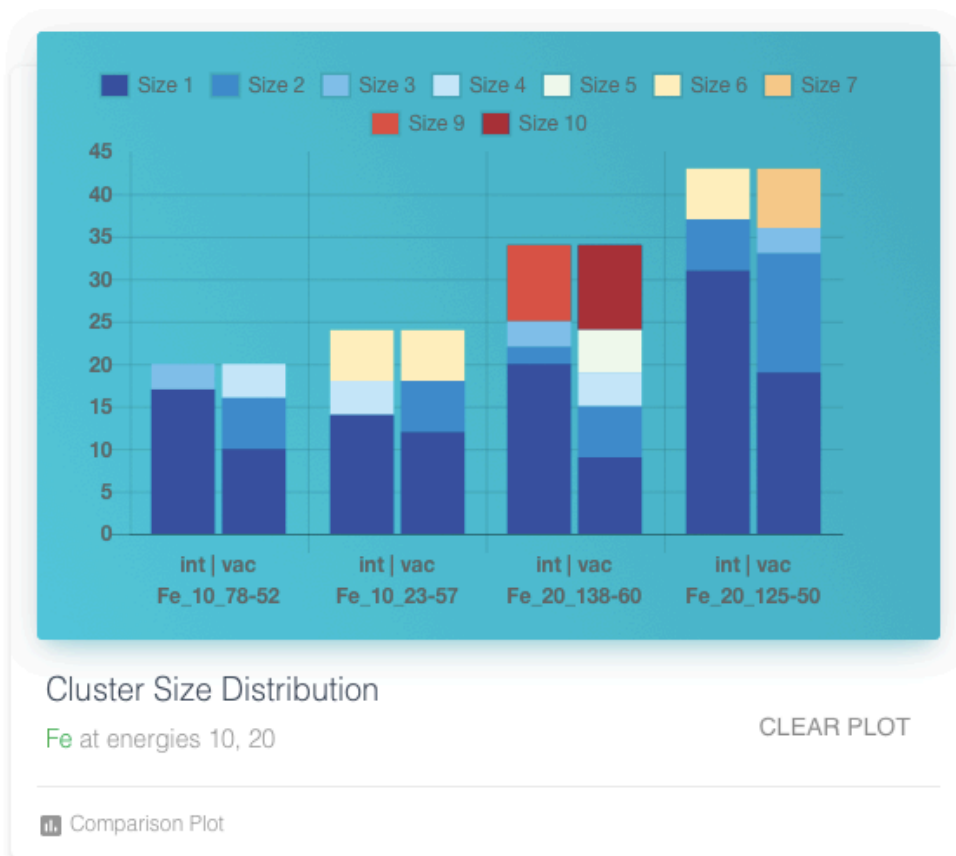
Figure 5: Cluster size distribution of the cascades selected from the main table.
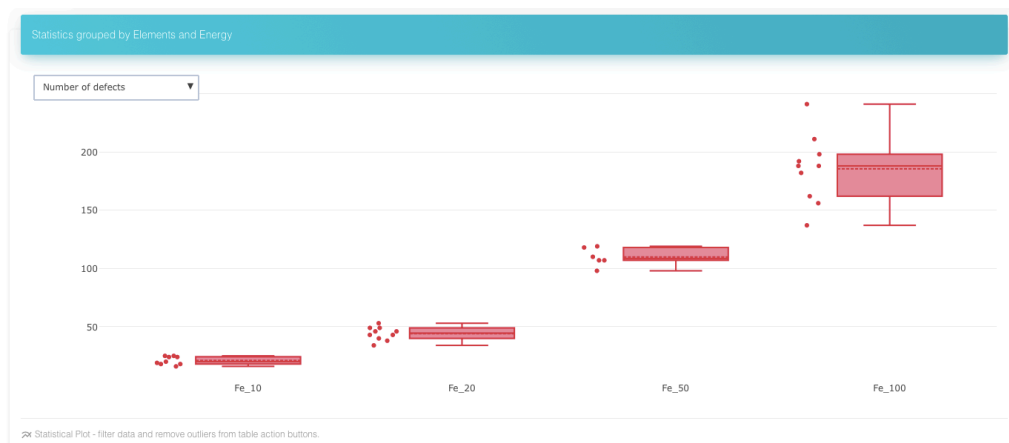

Figure 6: Number of defects over different energies in Fe. On mouse-over the boxes show mean, median, max and other statistics. Box plot for different properties can be plotted using the drop down menu. The statistics are aggregated for the rows filtered from the main table.
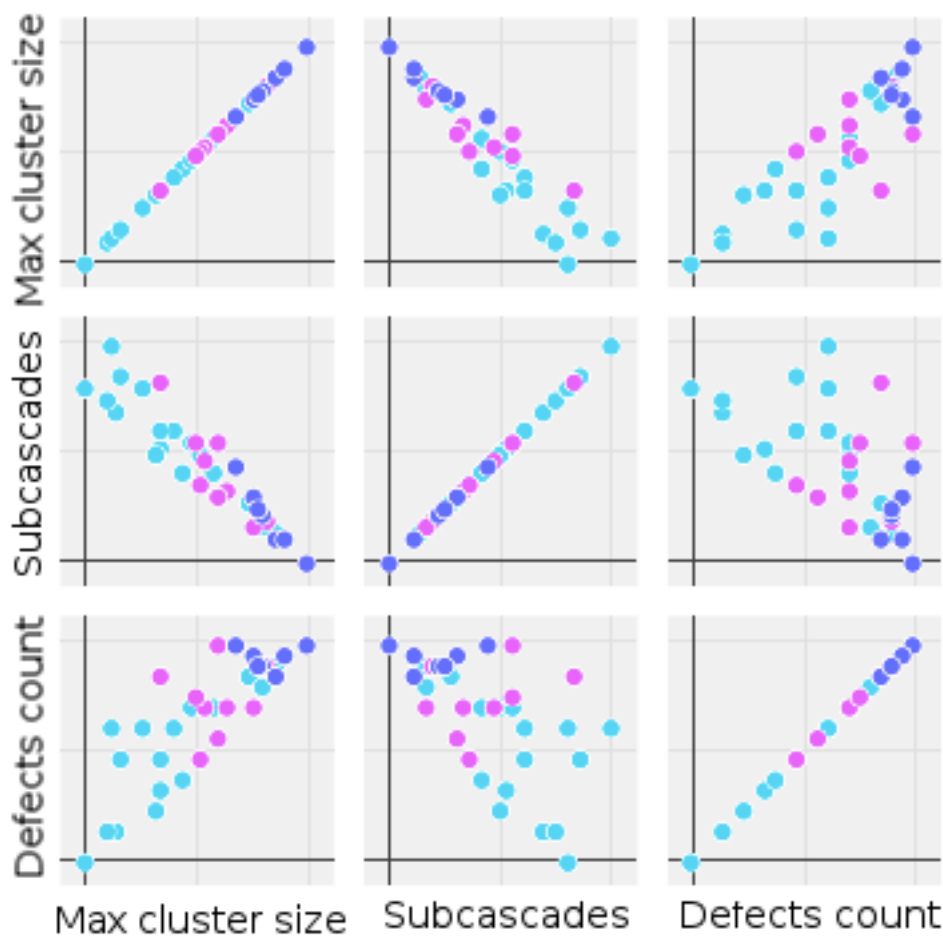
Figure 7: The scatter plot of each parameter against every other is plotted that helps in checking correlations and trends between the parameters such as number of defects, number of sub-cascades, in cascade clustering fraction etc. The color coding is for number of defects, which helps to see if a pair of parameters correlate to the number of defects.
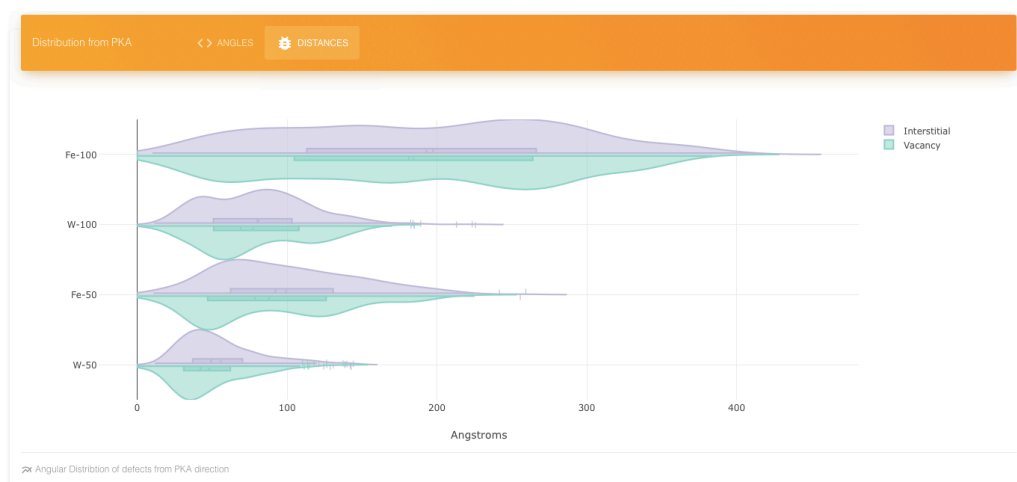

Figure 8: Shows the distance distribution of interstitials and vacancies from the PKA (primary knock-on atom) origin for Fe and W at two different energies.

Figure 9: The interactive plot shows the classification of cluster shapes on the left, each class having its own color. Each point represents a defect cluster. The two dimensional plot is generated using the dimensionality reduction algorithms UMAP (McInnes & Healy, 2018) or t-SNE (Maaten & Hinton, 2008) which place similar defect clusters nearby. The clusters are classified using HDBSCAN (Campello et al., 2013) unsupervised algorithm. Any cluster shape can be viewed on the right panel by clicking on a point on the left.

References

Becquart, C. S., Souidi, A., Domain, C., Hou, M., Malerba, L., & Stoller, R. E. (2006). Effect of displacement cascade structure and defect mobility on the growth of point defect clusters under irradiation. *Journal of Nuclear Materials*, *351*(1), 39–46. doi:10.1016/j.jnucmat.2006.02.022

Bhardwaj, U., Sand, A. E., & Warrier, M. (2018). Pattern matching and classification of clusters in collision cascades. *arXiv preprint arXiv:1811.10923*.

Bhardwaj, U., Sand, A. E., & Warrier, M. (2019). Classification of clusters in md simulations of collision cascades. http://dpc.nifs.ac.jp/dkato/MoD-PMI2019/. Retrieved July 7, 2019, from https://haptork.github.io/csaransh/presentation/index.html

Björkas, C., Nordlund, K., & Caturla, M. J. (2012). Influence of the picosecond defect distribution on damage accumulation in irradiated α-fe. *Phys. Rev. B*, *85*(2), 024105. doi:10.1103/PhysRevB.85.024105

Campello, R. J. G. B., Moulavi, D., & Sander, J. (2013). Density-based clustering based on hierarchical density estimates. In J. Pei, V. S. Tseng, L. Cao, H. Motoda, & G. Xu (Eds.), *Advances in knowledge discovery and data mining* (pp. 160–172). Berlin, Heidelberg: Springer Berlin Heidelberg. doi:10.1007/978-3-642-37456-2_14

Chartjs. (2014). Ceactjs. Retrieved October 9, 2018, from http://www.chartjs.org/

Facebook. (2013). Reactjs. Retrieved October 9, 2018, from https://reactjs.org

Golubov, S. I., Singh, B. N., & Trinkaus, H. (2000). Defect accumulation in fcc and bcc metals and alloys under cascade damage conditions – towards a generalisation of the production bias model. *Journal of Nuclear Materials*, *276*(1), 78–89. doi:10.1016/S0022-3115(99)00171-3

Hill, C. (2018). Managing large atomic and molecular data sets: HITRAN, exomol and cascadesdb. IAEA. Retrieved October 9, 2018, from https://www-amdis.iaea.org/Workshops/ICTP2018/Presentations/ICTP2018TalkHill.pdf

IAEA. (2018). IAEA challenge on materials for fusion - 2018. Retrieved October 9, 2018, from https://challenge.iaea.org/challenges/2018-NA-Mat-Fusion

Maaten, L. J. V., & Hinton, G. (2008). Visualizing high-dimensional data using t-sne. *Journal of Machine Learning Research*, *9*, 2579–2605.

McInnes, L., & Healy, J. (2018). Umap: Uniform manifold approximation and projection for dimension reduction. *arXiv preprint arXiv:1802.03426*.

Osetsky, Y., Bacon, D. J., Serra, A., Singh, B. N., & Golubov, S. I. (2000). Stability and mobility of defect clusters and dislocation loops in metals. *Journal of Nuclear Materials*, *276*(1), 65–77. doi:10.1016/S0022-3115(99)00170-1

Plotly. (2013). Plotly.js. Retrieved October 9, 2018, from https://plot.ly/javascript/

Singh, B. N., Golubov, S. I., Trinkaus, H., Serra, A., Osetsky, Y., & Barashev, A. V. (1997). Aspects of microstructure evolution under cascade damage conditions. *Journal of Nuclear Materials*, *251*, 107–122. doi:10.1016/S0022-3115(97)00244-4

Stoller, R. E. (2012). Primary radiation damage formation. In R. J. M. Konings (Ed.), *Comprehensive nuclear materials*. Elsevier. doi:10.1016/b978-0-08-056033-5.00027-6